

Article

Double Slit with an Einstein–Podolsky–Rosen Pair

Bar Y. Peled ^{1,†}, Amit Te'eni ^{2,†}, Danko Georgiev ³ , Eliahu Cohen ^{2,*}  and Avishy Carmi ¹ 

¹ Center for Quantum Information Science and Technology & Faculty of Engineering Sciences, Ben-Gurion University of the Negev, Beersheba 8410501, Israel; barp@post.bgu.ac.il (B.Y.P.); avcarmi@bgu.ac.il (A.C.)

² Faculty of Engineering and the Institute of Nanotechnology and Advanced Materials, Bar Ilan University, Ramat Gan 5290002, Israel; amitteeni@gmail.com

³ Institute for Advanced Study, 30 Vasilaki Papadopulu Str., Varna 9010, Bulgaria; danko.georgiev@mail.bg

* Correspondence: eliahu.cohen@biu.ac.il; Tel.: +972-3-738-4268

† These authors contributed equally to this work.

Received: 31 December 2019; Accepted: 20 January 2020; Published: 22 January 2020



Abstract: In this somewhat pedagogical paper we revisit complementarity relations in bipartite quantum systems. Focusing on continuous-variable systems, we examine the influential class of EPR-like states through a generalization to Gaussian states and present some new quantitative relations between entanglement and local interference within symmetric and asymmetric double-double-slit scenarios. This approach is then related to ancilla-based quantum measurements, and weak measurements in particular. Finally, we tie up the notions of distinguishability, predictability, coherence and visibility while drawing some specific connections between them.

Keywords: entanglement; interference; complementarity; continuous variables

1. Introduction

Distinguishability (or predictability) of paths in quantum interference experiments is closely linked with entanglement. For instance, to gain “which-path” information in a double-slit experiment, one should employ some kind of a measuring pointer (be it responsible for a strong, weak, partial measurement, etc.). The process of measuring the system’s path involves entangling it with the device. For simplicity, one could assume the system is already entangled with another, similar system (in the desired basis); then, the “which-path” information is contained in the correlations between the two systems—i.e., knowing which slit the particle went through in one system supplies information regarding which slit the other particle went through in the other system.

This approach was used by Jaeger et al. in [1], where the authors proposed a quantitative measure for two-particle interference, denoted by v_{12} , and proved a duality relation between one-particle interference visibility and two-particle interference visibility: $v_i^2 + v_{12}^2 \leq 1$ (where v_i denotes the i th particle’s interference visibility). This and other similar duality relations were studied in [2–5]. For general definitions and discussion of interferometric quantities in multiple-slit scenarios, please see Appendix A.

However, it seems to us that most of these works did not emphasize enough the state- and geometry-dependent quantitative relations between entanglement and interference of continuous variables (CV) such as position and momentum (or the corresponding quadratures of the electromagnetic field). The notions of nonlocality and entanglement in continuous-variable systems are intricate and subtle. Working in infinite-dimensional Hilbert spaces necessitates new theoretical methods (for entanglement and even quantumness quantification), new practical methods (like homodyne and heterodyne detectors), new tools (like Wigner functions, Q- and P-representations) and new conceptual ideas, but they also enable new opportunities for quantum communication and computation.

Since the first entangled state to reach world-wide acclaim was the continuous-variable EPR state [6,7], it is natural to ask whether complementarity relations similar to the aforementioned ones can be formulated in EPR-like states using continuous variables. However, in fact, our analysis here is more general, considering asymmetric configurations of Gaussian states, which reach the EPR state as a special, limiting case. Moreover, these CV states seem to offer richer relations between local and nonlocal observables than their discrete variables counterparts.

While discrete variable systems benefit from high-fidelity operations, they are limited by the imperfect generation and detection of single quanta (e.g., photons), as well as the absence of deterministic interactions of single quanta [8]. In contrast, encoding of quantum information in continuous variables can achieve deterministic, unconditional operation of quantum protocols, albeit at the expense of lower fidelities [8,9]. Although the high efficiency and unconditional preparation of CV entanglement is paid for with imperfection of the entanglement [10–12], the prepared Gaussian entangled states approach an ideal EPR state in the limit of infinite squeezing [13]. Thus, the practicality of continuous variables in quantum protocols is due to currently available highly efficient sources of squeezed laser light and existing techniques for preparing, unitarily manipulating, and measuring entangled quantum states, with the use of continuous quadrature amplitudes of the quantized electromagnetic field [10]. It is worth noting that in this paper we are mainly focused on theoretical aspects; experimental tests of complementarity using quantum optics may be found in [14–19], as well as a recent experiment using complementarity for nonlocal erasure of phase objects [20].

In Section 3 we define a family of EPR-like states, modeled using Gaussian wavepackets, where the strength of entanglement may be controlled by some parameter θ . We propose a quantitative measure for v_{12} , and find a relation analogous to the one-particle and two-particle interference complementarity. In the limit of zero-width Gaussian wavepackets (i.e., delta functions), our proposed system effectively reduces to a two-dimensional system, reproducing results similar to those shown in [1,2].

Furthermore, in Section 4 we define an “asymmetric” state, i.e., one where Alice’s system may have different parameters than Bob’s, in terms of how wide the slits are and to which extent the wavepacket is localized. Again, we derive an expression for the one-particle interference pattern visibility, and study its relation to the family of states we defined in Section 3. We conclude by discussing the generality of our work.

2. Model for Entangled Double-Slit Experiment Using Gaussian Wave Packets

In this section, we shall introduce a wavefunction which describes an *entangled* double-slit experiment, based on the famous EPR state. In the original EPR paper [6], the following state is presented

$$\psi_{EPR}(x_1, x_2) = \int_{-\infty}^{\infty} dx \delta(x_1 - x) \delta(x - x_2 + x_0). \tag{1}$$

For simplicity, we shall choose $x_0 = 0$. However, the above state does not reside in the Hilbert space L^2 of square integrable functions. Recalling that the delta function may be realized as a limit of Gaussian functions

$$\lim_{\Delta \rightarrow 0} \frac{1}{(\pi\Delta^2)^{1/2}} e^{-(x-x')^2/\Delta^2} = \delta(x - x'), \tag{2}$$

we substitute the delta functions in (1) with the LHS of (2), taken with finite Δ . This yields the following wavefunction

$$\psi_G(x_1, x_2) = \frac{a}{\pi} \int_{-\infty}^{\infty} dx e^{-a(x_1-x)^2} e^{-a(x_2-x)^2}, \tag{3}$$

where $a := 1/\Delta^2$. We note that (1) is reproduced in the limit $a \rightarrow \infty$. Now, we wish to pass both particles through a double slit, i.e., we are interested only in Gaussians centralized at one of two separate pairs

of slits, located at $x_i = \pm h_i$ for $i = 1, 2$ (see Figure 1 for an illustration). Thus, immediately after passing through the double slit, our initial wavefunction becomes

$$\psi(x_1, x_2) = A \left(e^{-a(x_1-h_1)^2} e^{-a(x_2-h_2)^2} + e^{-a(x_1+h_1)^2} e^{-a(x_2+h_2)^2} \right), \tag{4}$$

where $A = \sqrt{\frac{a/\pi}{1+e^{-2a(h_1^2+h_2^2)}}$ is a normalization factor.

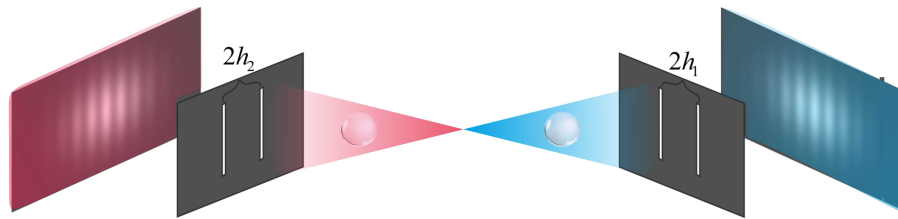


Figure 1. The proposed “double-double slit” setup: each particle of an entangled two-mode Gaussian state $\psi_\theta(x_1, x_2)$ (5) is sent through a double slit with a screen behind it. The amount of quantum entanglement between the two particles is controlled by a parameter $\theta \in [0, \frac{\pi}{4}]$. The experiment is repeated many times with the same initial state, and the positions where the particles hit the screen are registered to infer the one-particle and two-particle probability distributions. Generally, the distance between each pair of slits may vary. The plotted probability distributions on the screens are for $\theta = \frac{\pi}{4}$.

3. A Partially Entangled Double-Slit Experiment

In this section, we shall construct a model for a partially entangled double-slit experiment. Following Sec. III of [1], we start from (4), substitute $h_1 = h_2 = h$, construct an “opposite” wavefunction and take a normalized superposition of the two, yielding

$$\psi_\theta(x_1, x_2) = \frac{A_\theta}{A} [\psi(x_1, x_2) \cos \theta + \psi(x_1, -x_2) \sin \theta], \tag{5}$$

where $\theta \in [0, \frac{\pi}{4}]$ is a parameter controlling the amount of entanglement (note the entanglement strength decreases as θ increases), and

$$\frac{1}{A_\theta^2} = \frac{\pi}{a} \left[1 + 2e^{-2ah^2} \sin(2\theta) + e^{-4ah^2} \right]. \tag{6}$$

Propagation of a wave from the near to the far field transforms an initial state into its Fourier transform. Thus, the position wavefunction in some time t such that the wave has propagated to reach a screen located in the far field domain, is proportional to the initial momentum wavefunction. This implies the momentum wavefunction may be used to define and compute the interferometric quantities we wish to consider (i.e., one- and two-particle visibility). The momentum wavefunction and related derivations appear in Appendix B.1. The momentum probability density is

$$f_{p_1, \theta}(p_1) = \sqrt{\frac{2\pi}{a}} \pi B_\theta e^{-\frac{p_1^2}{2a}} \left(\left[1 + e^{-2ah^2} \cos(2hp_1) \right] + \sin(2\theta) \left[e^{-2ah^2} + \cos(2hp_1) \right] \right). \tag{7}$$

Taking a close look at (7), we notice that this probability density function is a sum of two parts: one which is independent of p_1 (up to normalization), and an oscillating part, with amplitude proportional to $\sin(2\theta)$. This allows us to write down expressions for the “envelopes” of these oscillations

$$env_+(p_1) = \pi \sqrt{\frac{2\pi}{a}} B_\theta e^{-\frac{p_1^2}{2a}} (1 + e^{-2ah^2}) [1 + \sin(2\theta)] \tag{8}$$

$$env_-(p_1) = \pi \sqrt{\frac{2\pi}{a}} B_\theta e^{-\frac{p_1^2}{2a}} (1 - e^{-2ah^2}) [1 - \sin(2\theta)]. \tag{9}$$

These were computed by substituting ± 1 for the cosine. However, it should be noted that because of the Gaussian, the extreme points of $f_{p_1,\theta}$ are not necessarily located in the extreme points of $\cos(2hp_1)$. Thus, the above envelopes are merely approximations. They are “good” approximations if the Gaussian changes much slower than the cosine, i.e., $ah^2 \gg 1$.

Now we wish to construct measures for the strength of interference. First, we compute the ratio between the envelopes

$$r_\theta \triangleq \frac{env_+(p_1)}{env_-(p_1)} = \frac{1 + e^{-2ah^2}}{1 - e^{-2ah^2}} \cdot \frac{1 + \sin(2\theta)}{1 - \sin(2\theta)} = \coth(ah^2) \frac{1 + \sin(2\theta)}{1 - \sin(2\theta)}, \tag{10}$$

where \coth denotes the hyperbolic cotangent. The envelopes also yield the well-known visibility measure

$$V_\theta = \frac{env_+(p_1) - env_-(p_1)}{env_+(p_1) + env_-(p_1)} = \frac{e^{-2ah^2} + \sin(2\theta)}{1 + e^{-2ah^2} \sin(2\theta)}. \tag{11}$$

Here, we note that $\sin(2\theta) \leq V_\theta \leq 1$, i.e., $\sin(2\theta)$ serves as a lower bound to the interference visibility. The more localized the Gaussian wavepackets, the closer the visibility is to $\sin(2\theta)$, which is also the value of the one-particle visibility in Sec. III of [1].

Next we compute the momentum joint probability distribution

$$\begin{aligned} f_{p_1 p_2, \theta}(p_1, p_2) &= \\ &= B_\theta \frac{\pi}{a} e^{-\frac{p_1^2 + p_2^2}{2a}} \left[1 + \cos^2 \theta \cos(2hp_+) + 2 \sin(2\theta) \cos(hp_+) \cos(hp_-) + \sin^2 \theta \cos(2hp_-) \right], \end{aligned} \tag{12}$$

where $p_\pm := p_1 \pm p_2$. Again, motivated by [1], we wish to define the two-particle visibility. To do so, we may construct the following “corrected” joint probability

$$\tilde{F}_\theta(p_1, p_2) = f_{p_1 p_2, \theta}(p_1, p_2) - f_{p_1, \theta}(p_1) f_{p_2, \theta}(p_2) + f_{p_1, \theta=0}(p_1) f_{p_2, \theta=0}(p_2),$$

where the “correction” term $f_{p_1, \theta=0}(p_1) f_{p_2, \theta=0}(p_2)$ is simply the value of $f_{p_1, \theta}(p_1) f_{p_2, \theta}(p_2)$ in the maximally entangled case, analogous to the term $\frac{1}{4}$ added in [1].

However, this is not precisely what we do. Instead, we take the added term with the same normalization factor B_θ as the subtracted one. This yields a much “nicer” expression with nearly the same value

$$\begin{aligned} \tilde{F}_\theta(p_+, p_-) &= \frac{e^{-\frac{p_+^2 + p_-^2}{4a}}}{C_\theta} \left[e^{4ah^2} + \cos^2(2\theta) + 2 \sin^2(2\theta) e^{2ah^2} \cos(hp_+) \cos(hp_-) \right] + \\ &+ \frac{1}{2} \frac{e^{-\frac{p_+^2 + p_-^2}{4a}}}{C_\theta} \left(1 + \cos^2(2\theta) e^{4ah^2} + \cos(2\theta) \left[1 + e^{4ah^2} + 2 \sin(2\theta) \right] \right) \cos(2hp_+) + \\ &+ \frac{1}{2} \frac{e^{-\frac{p_+^2 + p_-^2}{4a}}}{C_\theta} \left(1 + \cos^2(2\theta) e^{4ah^2} - \cos(2\theta) \left[1 + e^{4ah^2} + 2 \sin(2\theta) \right] \right) \cos(2hp_-), \end{aligned} \tag{13}$$

where $C_\theta := 8\pi a [\cosh(2ah^2) + \sin(2\theta)]^2$. Since the trigonometric functions are all non-negative in our domain of interest ($0 \leq \theta \leq \pi/4$), $\cos(2hp_+)$ has a larger amplitude than $\cos(2hp_-)$. Thus, the oscillations are dominated by p_+ , implying the envelopes are naturally defined by examining the

section $p_- = 0$, i.e., $p_1 = p_2$. The upper envelope is obtained by making the additional substitution $hp_+ = 2\pi n, n \in \mathbb{Z}$

$$env_+(p_+) = N_\theta e^{-\frac{p_+^2}{4a}} \left[2 + 2e^{4ah^2} - \sin^2(2\theta) (1 - e^{2ah^2})^2 \right], \tag{14}$$

and the lower envelope by $hp_+ = \pi/2 + 2\pi n, n \in \mathbb{Z}$

$$env_-(p_+) = N_\theta e^{-\frac{p_+^2}{4a}} \left(e^{4ah^2} - \cos(2\theta) \left[1 + e^{4ah^2} + 2 \sin(2\theta) - \cos(2\theta) \right] \right), \tag{15}$$

where $N_\theta = 1/C_\theta = \frac{1}{8\pi a [\cosh(2ah^2) + \sin(2\theta)]^2}$. Again, the envelopes are merely approximations, becoming more precise as ah^2 grows larger. Thus, we are motivated to produce even simpler expressions for the envelopes, by applying approximations valid for $ah^2 \gg 1$

$$env_+(p_+) \approx N_\theta e^{-\frac{p_+^2}{4a}} e^{4ah^2} \left[1 + \cos^2(2\theta) \right], \quad env_-(p_+) \approx N_\theta e^{-\frac{p_+^2}{4a}} e^{4ah^2} \left[1 - \cos(2\theta) \right]. \tag{16}$$

Thus, we obtain the following expression for the two-particle interference P_θ

$$P_\theta = \frac{\cos(2\theta) \cos^2 \theta}{1 - \cos(2\theta) \sin^2 \theta}. \tag{17}$$

Taking the simple expression for the visibility, $V_\theta = \sin(2\theta)$, we obtain

$$P_\theta^2 + V_\theta^2 \leq 1, \tag{18}$$

since $P_\theta \leq \cos(2\theta)$. We note that $\cos(2\theta)$ is the value of the two-particle interference visibility in Sec. III of [1]. The complementarity (18) is illustrated in Figure 2.

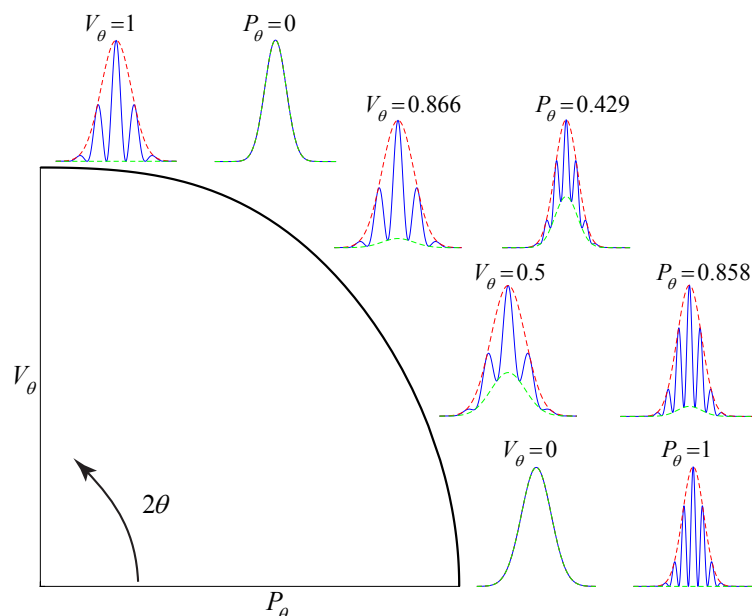


Figure 2. One-particle visibility V_θ (11) and two-particle visibility (predictability) P_θ (17) computed from the corresponding quantum probability distributions $f_{p_1, \theta}(p_1)$ (7) and $\tilde{F}_\theta(p_+, p_- = 0)$ (13) for different strengths of entanglement controlled by $\theta = 0, \pi/12, \pi/6$ and $\pi/4$. This plot illustrates the smooth transition from zero visibility and maximal predictability, to maximal visibility and zero predictability, as the entanglement diminishes. The bold line depicts a polar curve of $P_\theta^2 + V_\theta^2$.

The significance of inequalities of the form (18) is that they link a locally measured property (one-particle visibility) and a nonlocal property (two-particle visibility). A closely related inequality is illustrated in [21]

$$\left(\frac{\mathcal{B}}{2\sqrt{2}}\right)^2 + |\eta|^2 \leq 1, \tag{19}$$

where \mathcal{B} is the Bell-CHSH parameter—again a measure of nonlocality; and η is the quantum Pearson correlation between Alice’s observables, i.e., a property one may infer from measurements on Alice’s system.

4. Model for Asymmetric Entangled Double-Slit Experiment

In this section, we consider a generalization of (4). Recalling the aforementioned analogy between the double-double slit and two measurement pointers measuring the entangled pair of particles, we note that Bob’s system might be different from Alice’s system in several aspects. Bob’s pointer state could be implemented by an electron [22], cold ion [23] or any other quantum system. Moreover, his measuring system could correspond to variable strength coupling and could even have many degrees of freedom. However, we are only interested in one continuous degree of freedom out of the above giving rise to a pair of operators denoted by x_2, p_2 (not necessarily position and momentum), obeying the canonical commutation relations $[x_2, p_2] = i$. We therefore consider now asymmetric interactions corresponding to different measurements on the slits. Applying these interactions results in the following state

$$\psi(x_1, x_2) = M \left(e^{-a(x_1-h_1)^2} e^{-b(x_2-h_2)^2} + e^{-a(x_1+h_1)^2} e^{-b(x_2+h_2)^2} \right), \tag{20}$$

that is, Bob’s two slits are not in the same distance as Alice’s two slits, and his Gaussians have different widths than Alice’s (M is a normalization constant). The Wigner function of this state appears in Appendix B.2. We begin by writing down the wavefunction in momentum space:

$$\psi(p_1, p_2) = \frac{M}{2\sqrt{ab}} \left(e^{-\frac{1}{4a}(p_1+2ah_1i)^2 - ah_1^2} e^{-\frac{1}{4b}(p_2+2bh_2i)^2 - bh_2^2} + e^{-\frac{1}{4a}(p_1-2ah_1i)^2 - ah_1^2} e^{-\frac{1}{4b}(p_2-2bh_2i)^2 - bh_2^2} \right), \tag{21}$$

and computing the probability density of p_1 :

$$f_{p_1}(p_1) = \pi G \sqrt{\frac{2\pi}{a}} e^{-\frac{p_1^2}{2a}} \left[1 + e^{-2bh_2^2} \cos(2h_1p_1) \right]. \tag{22}$$

As before, (22) yields an expression for the upper (lower) envelope by substituting $\cos(2h_1p_1) = +1 (-1)$

$$env_{asymmetric}^{\pm} = \pi G \sqrt{\frac{2\pi}{a}} e^{-\frac{p_1^2}{2a}} \left[1 \pm e^{-2bh_2^2} \right]. \tag{23}$$

As in the previous section, these are approximations, valid for $ah_1^2 \gg 1$; however, we need not assume anything about b, h_2 . Again, we obtain a constant ratio

$$r_{asymmetric} = \frac{1 + e^{-2bh_2^2}}{1 - e^{-2bh_2^2}} = \coth(bh_2^2), \tag{24}$$

and constant visibility

$$V_{asymmetric} = e^{-2bh_2^2}. \tag{25}$$

We note that because of the asymmetry, the one-particle visibility for particle 1 (which is the one defined above) differs from the one-particle visibility for particle 2. Comparing (25) and (11), we wish to find a relation between the parameters determining the one-particle interference visibility. In the

“asymmetric” wavefunction, it is determined by b, h_2 , while in the theta-wavefunction it is determined by $a, h_1, \sin(2\theta)$. Taking the two expressions to be equal, we obtain

$$\frac{e^{-2ah_1^2} + \sin(2\theta)}{1 + \sin(2\theta) e^{-2ah_1^2}} = e^{-2bh_2^2}. \quad (26)$$

Solving for $\sin(2\theta)$ yields

$$\sin(2\theta) = \frac{e^{-2bh_2^2} - e^{-2ah_1^2}}{1 - e^{-2ah_1^2} e^{-2bh_2^2}} = \frac{V_{\text{asymmetric}} - e^{-2ah_1^2}}{1 - e^{-2ah_1^2} V_{\text{asymmetric}}}. \quad (27)$$

This also allows a simple way for Alice to generate a *purification* of her state, using only the parameters of her system and the interference visibility she measures. To put it more precisely, the state of the form (5) where θ is given by (27), yields the same single-particle Wigner function for Alice as the state (20) considered throughout this section (a proof appears in the Appendix B.3). Thus, (27) allows Alice to use any of the results obtained in the previous section, e.g., by computing the predictability.

We also note that Alice and Bob may switch roles and achieve similar results; this fact is manifested in (27) by noting the expression is invariant under permutation of the two particles.

5. Conclusions

In this work we derived a complementarity relation analogous to the one presented in [1], for a family of CV systems described by EPR-like states. This complementarity relation is sensitive to the parameters of the double-double-slit experiment, namely the width of each double slit and the separation between the slits. In addition, we have demonstrated that in CV systems, the “analog” visibility measures defined using interferometric envelopes, are closely related to the ones defined in previous works [1–4] with binary-outcome quantum probabilities.

Moreover, (27) allows application of this complementarity relation to any experiment where a CV is subjected to a binary-outcome measurement: one should have it evolve in a manner analogous to propagation of the double-slit wavefunction to the far field; afterwards, an interference pattern should be extracted, either an actual one or some analog; and finally, computation of the envelope-based visibility allow finding the “ θ ” and consequentially the predictability, thus inferring the strength of entanglement.

Additionally, common descriptions of the double-slit experiment usually consider two variants: one where a detector is placed next to one of the slits, and another variant where no detector is placed. However, since the process of measurement may be described by entangling the system and the measuring pointer, a natural way to describe *weak* measurements [24–27] or intermediate strength measurements [28,29] in a double-slit setting is by considering weak entanglement of the system and pointer. In this context, by varying the parameter θ which controls the amount of entanglement between the two particles in the initial state $\psi_\theta(x_1, x_2)$, this work may be also viewed as a model for “weak” variants of the double-slit experiment with continuous variables.

Finally, this paper strengthens and elucidates the tight relation between local and nonlocal correlations that we previously explored e.g., in [21,30,31].

Author Contributions: Conceptualization, D.G., E.C. and A.C.; Formal analysis, B.Y.P. and A.T.; Investigation, B.Y.P. and A.T.; Supervision, E.C. and A.C.; Validation, D.G., E.C. and A.C.; Writing original draft, B.Y.P., A.T. and D.G.; Writing review & editing, E.C. and A.C. All authors have read and agreed to the published version of the manuscript.

Funding: This research received no external funding.

Conflicts of Interest: The authors declare no conflict of interest.

Appendix A. Complementary Quantum Measures and Relations

Quantum particles can explore simultaneously multiple paths in a quantum coherent superposition. In general, the n alternative paths could be explicitly described with the use of quantum histories $\hat{Q}_1, \hat{Q}_2, \dots, \hat{Q}_n$, which are defined in history Hilbert space as tensor products of projection operators at multiple times, and the corresponding quantum probability amplitudes $\psi_1, \psi_2, \dots, \psi_n$ propagating along each path can be experimentally measured in the form of complex-valued sequential weak values [32]. Without loss of generality, after normalization it may be assumed that all given paths form a complete set of quantum histories $\sum_i |\psi_i|^2 = 1$. In the special case of n -slit interference setups, the sequential weak values reduce to ordinary weak values [24,25] with a single intermediate time at the slits, between the initial emission from the particle source and the final detection at a sensitive screen. The quantum coherence \mathcal{C} exhibited by each quantum particle in multi-slit setups could be manifested in visibility \mathcal{V} of interference fringes and is constrained by complementary relations to path predictability \mathcal{P} or path distinguishability \mathcal{D} , the latter demanding quantum entanglement with external path measuring devices.

Definition 1. Path distinguishability \mathcal{D} is defined with the use of external entanglement with measuring devices inserted on the paths. For the case of n paths, the distinguishability is [33–36]

$$\mathcal{D} = \sqrt{1 - \left(\frac{1}{n-1} \sum_{i \neq j} |\psi_i| |\psi_j| |\langle d_i | d_j \rangle| \right)^2} \tag{A1}$$

where different device states $|d_i\rangle, |d_j\rangle$ are normalized but not necessarily orthogonal [37]. For orthogonal states $\langle d_i | d_j \rangle = 0$, the path distinguishability is maximal, $\mathcal{D} = 1$.

For two equally likely paths, the path distinguishability reduces to

$$\mathcal{D} = \sqrt{1 - |\langle d_1 | d_2 \rangle|^2} \tag{A2}$$

Definition 2. Path predictability \mathcal{P} is defined without the need of external entanglement. The idea is that if two paths have different probabilities, one could predict which of the two paths has been taken with a success which exceeds a 50% random guess. For n paths, the predictability is [38]

$$\mathcal{P} = \sqrt{1 - \left(\frac{1}{n-1} \sum_{i \neq j} |\psi_i| |\psi_j| \right)^2} \tag{A3}$$

For two paths, the path predictability becomes [2]

$$\mathcal{P} = \left| |\psi_1|^2 - |\psi_2|^2 \right| \tag{A4}$$

Proof. Indeed, squaring both sides of (A3) and using $\sum_i |\psi_i|^2 = 1$, we obtain

$$\begin{aligned} \mathcal{P}^2 &= 1^2 - (2|\psi_1| |\psi_2|)^2 = \left(|\psi_1|^2 + |\psi_2|^2 \right)^2 - 4|\psi_1|^2 |\psi_2|^2 \\ &= |\psi_1|^4 + 2|\psi_1|^2 |\psi_2|^2 + |\psi_2|^4 - 4|\psi_1|^2 |\psi_2|^2 \\ &= \left(|\psi_1|^2 - |\psi_2|^2 \right)^2 \end{aligned}$$

Taking the square root on both sides gives (A4). \square

Definition 3. Path coherence \mathcal{C} quantifies the quantum interference between different paths [35]

$$\mathcal{C} = \frac{1}{n-1} \sum_{i \neq j} |\psi_i| |\psi_j| |\langle d_i | d_j \rangle| \tag{A5}$$

In the absence of any path detectors, $\langle d_i|d_j \rangle = 1$, the coherence reduces to

$$C = \frac{1}{n-1} \sum_{i \neq j} |\psi_i||\psi_j| \tag{A6}$$

Definition 4. Fringe visibility \mathcal{V} quantifies the contrast in observed interferometric distribution patterns and is given by

$$\mathcal{V} = \frac{I_{\max} - I_{\min}}{I_{\max} + I_{\min}} \tag{A7}$$

For two paths, the fringe visibility reduces to coherence

$$\mathcal{V} = \frac{2|\psi_1||\psi_2|}{|\psi_1|^2 + |\psi_2|^2} = 2|\psi_1||\psi_2| \tag{A8}$$

Proof. Consider using (A7) together with the Born rule for I_{\max} and I_{\min} to get

$$\begin{aligned} \mathcal{V} &= \frac{(|\psi_1| + |\psi_2|)^2 - (|\psi_1| - |\psi_2|)^2}{(|\psi_1| + |\psi_2|)^2 + (|\psi_1| - |\psi_2|)^2} \\ &= \frac{|\psi_1|^2 + |\psi_2|^2 + 2|\psi_1||\psi_2| - (|\psi_1|^2 + |\psi_2|^2 - 2|\psi_1||\psi_2|)}{|\psi_1|^2 + |\psi_2|^2 + 2|\psi_1||\psi_2| + |\psi_1|^2 + |\psi_2|^2 - 2|\psi_1||\psi_2|} \\ &= \frac{4|\psi_1||\psi_2|}{2|\psi_1|^2 + 2|\psi_2|^2} = 2|\psi_1||\psi_2| \end{aligned}$$

□

Even though for double-slit setups the fringe visibility reduces to coherence, for multiple slits fringe visibility is not a good measure of coherence. In fact, fringe visibility may increase with increasing decoherence as explicitly shown in a specific case of four-path interference by Qureshi [39].

The most general equality for multi-path interference of a quantum particle in the presence of path detectors is between path distinguishability and path coherence

$$\mathcal{D}^2 + C^2 = 1 \tag{A9}$$

Proof. Sum the squares of (A1) and (A5) to verify that the result is a unit. □

As a special case, where there are no external path measuring devices, $\langle d_i|d_j \rangle = 1$, we obtain path relationship between path predictability and path coherence

$$\mathcal{P}^2 + C^2 = 1 \tag{A10}$$

And if we further limit the setup only to two-path interference, the coherence can be replaced with fringe visibility

$$\mathcal{D}^2 + \mathcal{V}^2 = 1 \tag{A11}$$

$$\mathcal{P}^2 + \mathcal{V}^2 = 1 \tag{A12}$$

Recently, Qureshi proposed to assess n path coherence using a method of blocking most of the paths to measure interference visibilities of path pairs [40]. It should be noted that the moduli of quantum probability amplitudes $|\psi_i|$ for n paths could be determined with only n measurements of individual path probabilities, $|\psi_i| = \sqrt{P_i}$. However, to determine orthogonality relations between external path detectors $|\langle d_i|d_j \rangle|$ one would need $n^2 - n$ pairs of measurements. In essence, Qureshi's proposal is to combine both types of measurements and assess $n^2 - n$ pairs of visibilities $|\psi_i||\psi_j||\langle d_i|d_j \rangle|$, which will then be summed according to Formula (A5).

Appendix B. Computations and Wigner Functions

Appendix B.1. The Wigner Function for a Partially Entangled Double-Slit Experiment

Let us write down the Wigner function of the state (5):

$$\begin{aligned}
 W_\theta(x_1, x_2, p_1, p_2) = & B_\theta \cos^2 \theta \left(g_1^- g_2^- + g_1^+ g_2^+ + 2g_1^0 g_2^0 \cos [2h(p_1 + p_2)] \right) + \\
 & + B_\theta \sin(2\theta) \left[\cos(2hp_1) g_1^0 (g_2^- + g_2^+) + \cos(2hp_2) g_2^0 (g_1^- + g_1^+) \right] \quad (A13) \\
 & + B_\theta \sin^2 \theta \left(g_1^- g_2^+ + g_1^+ g_2^- + 2g_1^0 g_2^0 \cos [2h(p_1 - p_2)] \right)
 \end{aligned}$$

where $g_i^\pm := e^{-2a(x_i \pm h)^2} e^{-\frac{p_i^2}{2a}}$, $g_i^0 := e^{-2ax_i^2} e^{-\frac{p_i^2}{2a}}$ and $B_\theta := \frac{A_0^2}{2\pi a}$. Now we shall compute the “partial” Wigner function of x_1, p_1

$$\begin{aligned}
 W_{1,\theta}(x_1, p_1) & := \int dx_2 \int dp_2 W_\theta(x_1, x_2, p_1, p_2) = \\
 & = \pi B_\theta \left[1 + e^{-2ah^2} \sin(2\theta) \right] (g_1^- + g_1^+) + 2\pi B_\theta \left[e^{-2ah^2} + \sin(2\theta) \right] g_1^0 \cos(2hp_1) \quad (A14)
 \end{aligned}$$

We note that for $\theta = \pi/4$ we have

$$W_{1,\theta=\pi/4}(x_1, p_1) = \frac{1}{2\pi \left(1 + e^{-2ah^2} \right)} \left[g_1^- + g_1^+ + 2g_1^0 \cos(2hp_1) \right] \quad (A15)$$

which is equal to the Wigner function for a single-particle double-slit system. The momentum probability density is computed by

$$f_{p_1,\theta}(p_1) = \int dx_1 W_{1,\theta}(x_1, p_1) \quad (A16)$$

and the momentum *joint* probability distribution is

$$\begin{aligned}
 f_{p_1 p_2,\theta}(p_1, p_2) & := \int dx_1 \int dx_2 W_\theta(x_1, x_2, p_1, p_2) \quad (A17) \\
 & = B_\theta \frac{\pi}{a} e^{-\frac{p_1^2 + p_2^2}{2a}} \left\{ 1 + \cos^2 \theta \cos [2h(p_1 + p_2)] + \sin(2\theta) [\cos(2hp_1) + \cos(2hp_2)] + \right. \\
 & \quad \left. + \sin^2 \theta \cos [2h(p_1 - p_2)] \right\} \\
 & = B_\theta \frac{\pi}{a} e^{-\frac{p_1^2 + p_2^2}{2a}} \left\{ 1 + \cos(2hp_1) \cos(2hp_2) - \cos(2\theta) \sin(2hp_1) \sin(2hp_2) + \right. \\
 & \quad \left. + \sin(2\theta) [\cos(2hp_1) + \cos(2hp_2)] \right\} \\
 & = B_\theta \frac{\pi}{a} e^{-\frac{p_1^2 + p_2^2}{2a}} \left[1 + \cos^2 \theta \cos(2hp_+) + 2 \sin(2\theta) \cos(hp_+) \cos(hp_-) + \right. \\
 & \quad \left. + \sin^2 \theta \cos(2hp_-) \right]. \quad (A18)
 \end{aligned}$$

The “corrected” momentum joint probability is defined by

$$\begin{aligned}
 \tilde{F}_\theta(p_1, p_2) &:= f_{p_1 p_2, \theta}(p_1, p_2) - f_{p_1, \theta}(p_1) f_{p_2, \theta}(p_2) + \frac{B_\theta}{B_{\theta=0}} f_{p_1, \theta=0}(p_1) f_{p_2, \theta=0}(p_2) = \\
 &= + \frac{e^{-\frac{p_1^2 + p_2^2}{2a}}}{C_\theta} \left[e^{4ah^2} + \cos(2hp_1) \cos(2hp_2) + \cos^2(2\theta) \right] + \\
 &+ \frac{e^{-\frac{p_1^2 + p_2^2}{2a}}}{C_\theta} \left[\sin^2(2\theta) e^{2ah^2} [\cos(2hp_1) + \cos(2hp_2)] - \cos(2\theta) \sin(2hp_1) \sin(2hp_2) \right] + \\
 &+ \frac{e^{-\frac{p_1^2 + p_2^2}{2a}}}{C_\theta} \left[\cos^2(2\theta) e^{4ah^2} \cos(2hp_1) \cos(2hp_2) - \cos(2\theta) e^{4ah^2} \sin(2hp_1) \sin(2hp_2) \right] + \\
 &- \frac{e^{-\frac{p_1^2 + p_2^2}{2a}}}{C_\theta} \sin(4\theta) e^{2ah^2} \sin(2hp_1) \sin(2hp_2) = \\
 &= + \frac{e^{-\frac{p_+^2 + p_-^2}{4a}}}{C_\theta} \left(e^{4ah^2} + \cos^2(2\theta) + \frac{1}{2} \left[1 + \cos^2(2\theta) e^{4ah^2} \right] [\cos(2hp_+) + \cos(2hp_-)] \right) + \tag{A19} \\
 &+ 2e^{-\frac{p_+^2 + p_-^2}{4a}} \sin^2(2\theta) e^{2ah^2} \cos(hp_+) \cos(hp_-) + \\
 &- \frac{1}{2} \frac{e^{-\frac{p_+^2 + p_-^2}{4a}}}{C_\theta} \cos(2\theta) \left[1 + e^{4ah^2} + 2 \sin(2\theta) \right] [\cos(2hp_-) - \cos(2hp_+)] = \\
 &= + \frac{e^{-\frac{p_+^2 + p_-^2}{4a}}}{C_\theta} \left[e^{4ah^2} + \cos^2(2\theta) + 2 \sin^2(2\theta) e^{2ah^2} \cos(hp_+) \cos(hp_-) \right] + \\
 &+ \frac{1}{2} \frac{e^{-\frac{p_+^2 + p_-^2}{4a}}}{C_\theta} \left(1 + \cos^2(2\theta) e^{4ah^2} + \cos(2\theta) \left[1 + e^{4ah^2} + 2 \sin(2\theta) \right] \right) \cos(2hp_+) + \\
 &+ \frac{1}{2} \frac{e^{-\frac{p_+^2 + p_-^2}{4a}}}{C_\theta} \left(1 + \cos^2(2\theta) e^{4ah^2} - \cos(2\theta) \left[1 + e^{4ah^2} + 2 \sin(2\theta) \right] \right) \cos(2hp_-).
 \end{aligned}$$

Substituting $p_- = 0$, we obtain

$$\begin{aligned}
 \tilde{F}_\theta(p_+, p_- = 0) &= \frac{e^{-\frac{p_+^2}{4a}}}{C_\theta} \left[e^{4ah^2} + \cos^2(2\theta) + 2 \sin^2(2\theta) e^{2ah^2} \cos(hp_+) \right] + \\
 &+ \frac{1}{2} \frac{e^{-\frac{p_+^2}{4a}}}{C_\theta} \left(1 + \cos^2(2\theta) e^{4ah^2} + \cos(2\theta) \left[1 + e^{4ah^2} + 2 \sin(2\theta) \right] \right) \cos(2hp_+) + \tag{A20} \\
 &+ \frac{1}{2} \frac{e^{-\frac{p_+^2}{4a}}}{C_\theta} \left(1 + \cos^2(2\theta) e^{4ah^2} - \cos(2\theta) \left[1 + e^{4ah^2} + 2 \sin(2\theta) \right] \right).
 \end{aligned}$$

Appendix B.2. The Wigner Function for an Asymmetric Double-Slit Experiment

The Wigner function corresponding to (20) is:

$$W(x_1, x_2, p_1, p_2) = G (\gamma_1^- \gamma_2^- + \gamma_1^+ \gamma_2^+) + 2G \gamma_1^0 \gamma_2^0 \cos(2h_1 p_1 + 2h_2 p_2) \tag{A21}$$

where $\gamma_1^\pm := e^{-2a(x_1 \pm h_1)^2} e^{-\frac{p_1^2}{2a}}$, $\gamma_2^\pm := e^{-2b(x_2 \pm h_2)^2} e^{-\frac{p_2^2}{2b}}$, $\gamma_1^0 := e^{-2ax_1^2} e^{-\frac{p_1^2}{2a}}$, $\gamma_2^0 := e^{-2bx_2^2} e^{-\frac{p_2^2}{2b}}$ and $G := \frac{M^2}{2\pi\sqrt{ab}}$. The “partial” Wigner function is:

$$W_1(x_1, p_1) := \int dx_2 \int dp_2 W(x_1, x_2, p_1, p_2) = \pi G \left[\gamma_1^- + \gamma_1^+ + 2e^{-2bh_2^2} \gamma_1^0 \cos(2h_1 p_1) \right]. \tag{A22}$$

Appendix B.3. Purification of Alice’s Subsystem

Suppose Alice is entangled with Bob in an asymmetric manner, and has no knowledge of anything outside her system; however, she knows the parameters a, h_1 . She performs interference experiments, obtains an interference pattern and uses it to compute $V_{asymmetric}$. Here we demonstrate she can always purify her state - i.e., write down a pure “Alice-Bob” state of the form (5) yielding the same one-particle Wigner function for Alice.

Our claim here, is that the state (5) where θ is a solution of (27) satisfies the above requirement. Indeed, substituting (26) in (A22) yields:

$$\begin{aligned}
 W_{1,asym}(x_1, p_1) &= \pi G \left[g_1^- + g_1^+ + 2g_1^0 \frac{e^{-2ah_1^2} + \sin(2\theta)}{1 + \sin(2\theta)e^{-2ah_1^2}} \cos(2h_1 p_1) \right] = \\
 &= \frac{\pi G}{1 + \sin(2\theta)e^{-2ah_1^2}} \left(\left[1 + e^{-2ah_1^2} \sin(2\theta) \right] (g_1^- + g_1^+) + 2 \left[e^{-2ah_1^2} + \sin(2\theta) \right] g_1^0 \cos(2h_1 p_1) \right)
 \end{aligned}
 \tag{A23}$$

which is identical to (A14) up to normalization, implying it should be completely identical, thus concluding the proof.

References

1. Jaeger, G.; Horne, M.A.; Shimony, A. Complementarity of one-particle and two-particle interference. *Phys. Rev. A* **1993**, *48*, 1023–1027. [[CrossRef](#)] [[PubMed](#)]
2. Greenberger, D.M.; Yasin, A. Simultaneous wave and particle knowledge in a neutron interferometer. *Phys. Lett. A* **1988**, *128*, 391–394. [[CrossRef](#)]
3. Jaeger, G.; Shimony, A.; Vaidman, L. Two interferometric complementarities. *Phys. Rev. A* **1995**, *51*, 54–67. [[CrossRef](#)] [[PubMed](#)]
4. Englert, B.G. Fringe visibility and which-way information: an inequality. *Phys. Rev. Lett.* **1996**, *77*, 2154–2157. [[CrossRef](#)] [[PubMed](#)]
5. Franson, J.D. Bell inequality for position and time. *Phys. Rev. Lett.* **1989**, *62*, 2205–2208. [[CrossRef](#)] [[PubMed](#)]
6. Einstein, A.; Podolsky, B.; Rosen, N. Can quantum-mechanical description of physical reality be considered complete? *Phys. Rev.* **1935**, *47*, 777–780. [[CrossRef](#)]
7. Schrödinger, E. Discussion of probability relations between separated systems. *Math. Proc. Camb. Philos. Soc.* **1935**, *31*, 555–563. [[CrossRef](#)]
8. Masada, G.; Miyata, K.; Politi, A.; Hashimoto, T.; O'Brien, J.L.; Furusawa, A. Continuous-variable entanglement on a chip. *Nat. Photonics* **2015**, *9*, 316–319. [[CrossRef](#)]
9. Pirandola, S.; Eisert, J.; Weedbrook, C.; Furusawa, A.; Braunstein, S.L. Advances in quantum teleportation. *Nat. Photonics* **2015**, *9*, 641–652. [[CrossRef](#)]
10. Braunstein, S.L.; van Loock, P. Quantum information with continuous variables. *Rev. Mod. Phys.* **2005**, *77*, 513–577. [[CrossRef](#)]
11. Eisert, J.; Plenio, M.B. Introduction to the basics of entanglement theory in continuous-variable systems. *Int. J. Quantum Inf.* **2003**, *1*, 479–506. [[CrossRef](#)]
12. Serafini, A., Entanglement of continuous variable systems. In *Quantum Continuous Variables: A Primer of Theoretical Methods*; CRC Press: Boca Raton, FL, USA, 2017; Chapter 7; pp. 171–222. [[CrossRef](#)]
13. Adesso, G.; Illuminati, F. Entanglement in continuous-variable systems: recent advances and current perspectives. *J. Phys. A* **2007**, *40*, 7821–7880. [[CrossRef](#)]
14. Scully, M.O.; Englert, B.G.; Walther, H. Quantum optical tests of complementarity. *Nature* **1991**, *351*, 111–116. [[CrossRef](#)]
15. Englert, B.G.; Walther, H.; Scully, M.O. Quantum optical Ramsey fringes and complementarity. *Appl. Phys. B* **1992**, *54*, 366–368. [[CrossRef](#)]
16. Herzog, T.J.; Kwiat, P.G.; Weinfurter, H.; Zeilinger, A. Complementarity and the quantum eraser. *Phys. Rev. Lett.* **1995**, *75*, 3034–3037. [[CrossRef](#)]
17. Bertet, P.; Osnaghi, S.; Rauschenbeutel, A.; Nogues, G.; Auffeves, A.; Brune, M.; Raimond, J.M.; Haroche, S. A complementarity experiment with an interferometer at the quantum—Classical boundary. *Nature* **2001**, *411*, 166–170. [[CrossRef](#)]
18. Braig, C.; Zarda, P.; Kurtsiefer, C.; Weinfurter, H. Experimental demonstration of complementarity with single photons. *Appl. Phys. B* **2003**, *76*, 113–116. [[CrossRef](#)]
19. Jacques, V.; Lai, N.D.; Dréau, A.; Zheng, D.; Chauvat, D.; Treussart, F.; Grangier, P.; Roch, J.F. Illustration of quantum complementarity using single photons interfering on a grating. *New J. Phys.* **2008**, *10*, 123009. [[CrossRef](#)]
20. Gao, L.; Zhang, Y.; Cohen, E.; Elitzur, A.C.; Karimi, E. Nonlocal quantum erasure of phase objects. *Appl. Phys. Lett.* **2019**, *115*, 051102. [[CrossRef](#)]

21. Carmi, A.; Cohen, E. Relativistic independence bounds nonlocality. *Sci. Adv.* **2019**, *5*, eaav8370. [[CrossRef](#)]
22. Pan, Y.; Cohen, E.; Karimi, E.; Gover, A.; Kaminer, I.; Aharonov, Y. Weak measurement, projective measurement and quantum-to-classical transitions in electron-photon interactions. *arXiv* **2019**, arXiv:1910.11685.
23. Pan, Y.; Zhang, J.; Cohen, E.; Wu, C.W.; Chen, P.X.; Davidson, N. Observation of the weak-to-strong transition of quantum measurement in trapped ions. *arXiv* **2019**, arXiv:1910.11684.
24. Aharonov, Y.; Albert, D.Z.; Vaidman, L. How the result of a measurement of a component of the spin of a spin- $\frac{1}{2}$ particle can turn out to be 100. *Phys. Rev. Lett.* **1988**, *60*, 1351–1354. [[CrossRef](#)] [[PubMed](#)]
25. Tamir, B.; Cohen, E. Introduction to weak measurements and weak values. *Quanta* **2013**, *2*, 7–17. [[CrossRef](#)]
26. Dressel, J.; Malik, M.; Miatto, F.M.; Jordan, A.N.; Boyd, R.W. Understanding quantum weak values: basics and applications. *Rev. Mod. Phys.* **2014**, *86*, 307–316. [[CrossRef](#)]
27. Vaidman, L.; Ben-Israel, A.; Dziewior, J.; Knips, L.; Weiß, M.; Meinecke, J.; Schwemmer, C.; Ber, R.; Weinfurter, H. Weak value beyond conditional expectation value of the pointer readings. *Phys. Rev. A* **2017**, *96*, 032114. [[CrossRef](#)]
28. Piacentini, F.; Avella, A.; Gramegna, M.; Lussana, R.; Villa, F.; Tosi, A.; Brida, G.; Degiovanni, I.P.; Genovese, M. Investigating the effects of the interaction intensity in a weak measurement. *Sci. Rep.* **2017**, *8*, 6959. [[CrossRef](#)]
29. Dziewior, J.; Knips, L.; Farfurnik, D.; Senkalla, K.; Benshalom, N.; Efroni, J.; Meinecke, J.; Bar-Ad, S.; Weinfurter, H.; Vaidman, L. Universality of local weak interactions and its application for interferometric alignment. *Proc. Natl. Acad. Sci. USA* **2019**, *116*, 2881–2890. [[CrossRef](#)]
30. Carmi, A.; Cohen, E. On the significance of the quantum mechanical covariance matrix. *Entropy* **2018**, *20*, 500. [[CrossRef](#)]
31. Carmi, A.; Herasymenko, Y.; Cohen, E.; Snizhko, K. Bounds on nonlocal correlations in the presence of signaling and their application to topological zero modes. *New J. Phys.* **2019**, *21*, 073032. [[CrossRef](#)]
32. Georgiev, D.; Cohen, E. Probing finite coarse-grained virtual Feynman histories with sequential weak values. *Phys. Rev. A* **2018**, *97*, 052102. [[CrossRef](#)]
33. Zhang, S.; Feng, Y.; Sun, X.; Ying, M. Upper bound for the success probability of unambiguous discrimination among quantum states. *Phys. Rev. A* **2001**, *64*, 062103. [[CrossRef](#)]
34. Qiu, D. Upper bound on the success probability for unambiguous discrimination. *Phys. Lett. A* **2002**, *303*, 140–146. [[CrossRef](#)]
35. Bera, M.N.; Qureshi, T.; Siddiqui, M.A.; Pati, A.K. Duality of quantum coherence and path distinguishability. *Phys. Rev. A* **2015**, *92*, 012118. [[CrossRef](#)]
36. Qureshi, T.; Siddiqui, M.A. Wave-particle duality in N -path interference. *Ann. Phys.* **2017**, *385*, 598–604. [[CrossRef](#)]
37. Siddiqui, M.A.; Qureshi, T. A nonlocal wave-particle duality. *Quantum Stud. Math. Found.* **2016**, *3*, 115–122. [[CrossRef](#)]
38. Roy, P.; Qureshi, T. Path predictability and quantum coherence in multi-slit interference. *Phys. Scr.* **2019**, *94*, 095004. [[CrossRef](#)]
39. Qureshi, T. Coherence, interference and visibility. *Quanta* **2019**, *8*, 24–35. [[CrossRef](#)]
40. Qureshi, T. Interference visibility and wave-particle duality in multipath interference. *Phys. Rev. A* **2019**, *100*, 042105. [[CrossRef](#)]

